Santa Clara University
Scholar Commons

6-23-2004

Emissions pathways, climate change, and impacts on California

Katherine Hayhoe

Daniel Cayan

Christopher B. Field

Peter C. Frumhoff

Edwin P. Maurer
Santa Clara University, emaurer@scu.edu

See next page for additional authors

Follow this and additional works at: http://scholarcommons.scu.edu/ceng

Part of the Civil and Environmental Engineering Commons

Authors

Katherine Hayhoe, Daniel Cayan, Christopher B. Field, Peter C. Frumhoff, Edwin P. Maurer, Norman L. Miller, Susanne C. Moser, Stephen H. Schneider, Kimberly Nicholas Cahill, Elsa E. Cleland, Larry Dale, Ray Drapek, R. Hanemann, Laurence S. Kalkstein, James Lenihan, Claire K. Lunch, Ronald P. Nielson, Scott C. Sheridan, and Julia H. Verville

Emissions pathways, climate change, and impacts on California

Katharine Hayhoe[a,b], Daniel Cayan[c], Christopher B. Field[d], Peter C. Frumhoff[e], Edwin P. Maurer[f], Norman L. Miller[g], Susanne C. Moser[h], Stephen H. Schneider[i], Kimberly Nicholas Cahill[d], Elsa E. Cleland[d], Larry Dale[g], Ray Drapek[j], R. Michael Hanemann[k], Laurence S. Kalkstein[l], James Lenihan[j], Claire K. Lunch[d], Ronald P. Neilson[j], Scott C. Sheridan[m], and Julia H. Verville[e]

[a]ATMOS Research and Consulting, 809 West Colfax Avenue, South Bend, IN 46601; [c]Climate Research Division, The Scripps Institution of Oceanography, and Water Resources Division, U.S. Geological Survey, 9500 Gilman Drive, La Jolla, CA 92093-0224; [d]Department of Global Ecology, Carnegie Institution of Washington, 260 Panama Street, Stanford, CA 94305; [e]Union of Concerned Scientists, Two Brattle Square, Cambridge, MA 02238; [f]Civil Engineering Department, Santa Clara University, Santa Clara, CA 95053; [g]Atmosphere and Ocean Sciences Group, Earth Sciences Division, Lawrence Berkeley National Laboratory, 1 Cyclotron Road, Berkeley, CA 94720; [h]Environmental and Societal Impacts Group, National Center for Atmospheric Research, P.O. Box 3000, Boulder, CO 80307; [i]Department of Biological Sciences and Institute for International Studies, Stanford University, Stanford, CA 94305; [j]Corvallis Forestry Sciences Laboratory, U.S. Department of Agriculture Forest Service, 3200 SW Jefferson Way, Corvallis, OR 97331; [k]Department of Agricultural and Resource Economics, University of California, Berkeley, CA 94720; [l]Center for Climatic Research, Department of Geography, University of Delaware, Newark, DE 19716; and [m]Department of Geography, Kent State University, Kent, OH 44242

The magnitude of future climate change depends substantially on the greenhouse gas emission pathways we choose. Here we explore the implications of the highest and lowest Intergovernmental Panel on Climate Change emissions pathways for climate change and associated impacts in California. Based on climate projections from two state-of-the-art climate models with low and medium sensitivity (Parallel Climate Model and Hadley Centre Climate Model, version 3, respectively), we find that annual temperature increases nearly double from the lower B1 to the higher A1fi emissions scenario before 2100. Three of four simulations also show greater increases in summer temperatures as compared with winter. Extreme heat and the associated impacts on a range of temperature-sensitive sectors are substantially greater under the higher emissions scenario, with some interscenario differences apparent before midcentury. By the end of the century under the B1 scenario, heatwaves and extreme heat in Los Angeles quadruple in frequency while heat-related mortality increases two to three times; alpine/subalpine forests are reduced by 50–75%; and Sierra snowpack is reduced 30–70%. Under A1fi, heatwaves in Los Angeles are six to eight times more frequent, with heat-related excess mortality increasing five to seven times; alpine/subalpine forests are reduced by 75–90%; and snowpack declines 73–90%, with cascading impacts on runoff and streamflow that, combined with projected modest declines in winter precipitation, could fundamentally disrupt California's water rights system. Although interscenario differences in climate impacts and costs of adaptation emerge mainly in the second half of the century, they are strongly dependent on emissions from preceding decades.

California, with its diverse range of climate zones, limited water supply, and economic dependence on climate-sensitive industries such as agriculture, provides a challenging test case to evaluate impacts of regional-scale climate change under alternative emissions pathways. As characterized by the Intergovernmental Panel on Climate Change, demographic, socioeconomic, and technological assumptions underlying long-term emissions scenarios vary widely (1). Previous studies have not systematically examined the difference between projected regional-scale changes in climate and associated impacts across scenarios. Nevertheless, such information is essential to evaluate the potential for and costs of adaptation associated with alternative emissions futures and to inform mitigation policies (2).

Here, we examine a range of potential climate futures that represent uncertainties in both the physical sensitivity of current climate models and divergent greenhouse gas emissions pathways. Two global climate models, the low-sensitivity National Center for Atmospheric Research/Department of Energy Par-

allel Climate Model (PCM) (3) and the medium-sensitivity U.K. Met Office Hadley Centre Climate Model, version 3 (HadCM3), model (4, 5) are used to calculate climate change resulting from the SRES (Special Report on Emission Scenarios) B1 (lower) and A1fi (higher) emissions scenarios (1). These scenarios bracket a large part of the range of Intergovernmental Panel on Climate Change nonintervention emissions futures with atmospheric concentrations of CO_2 reaching $\approx$550 ppm (B1) and $\approx$970 ppm (A1fi) by 2100 (see *Emissions Scenarios* in *Supporting Text*, which is published as supporting information on the PNAS web site). Although the SRES scenarios do not explicitly assume any specific climate mitigation policies, they do serve as useful proxies for assessing the outcome of emissions pathways that could result from different emissions reduction policies. The scenarios at the lower end of the SRES family are comparable to emissions pathways that could be achieved by relatively aggressive emissions reduction policies, whereas those at the higher end are comparable to emissions pathways that would be more likely to occur in the absence of such policies.

Climate Projections

Downscaling Methods. For hydrological and agricultural analyses, HadCM3 and PCM output was statistically downscaled to a $1/8°$ grid ($\approx$150 km^2) (6) and to individual weather stations (7) for analyses of temperature and precipitation extremes and health impacts. Downscaling to the $1/8°$ grid used an empirical statistical technique that maps the probability density functions for modelled monthly precipitation and temperature for the climatological period (1961–1990) onto those of gridded historical observed data, so the mean and variability of observations are reproduced by the climate model data. The bias correction and spatial disaggregation technique is one originally developed for adjusting General Circulation Model output for long-range streamflow forecasting (6), later adapted for use in studies examining the hydrologic impacts of climate change (8), and compares favorably to different statistical and dynamic downscaling techniques (9) in the context of hydrologic impact studies.

Station-level downscaling for analyses of temperature and precipitation extremes and health impacts used a deterministic method in which grid-cell values of temperatures and precipi-

---

Table 1. Summary of midcentury (2020–2049) and end-of-century (2070–2099) climate and impact projections for the HadCM3 and PCM B1 and A1fi scenarios

| | | | 2020–2049 | | | | 2070–2099 | | | |
| | | | PCM | | HadCM3 | | PCM | | HadCM3 | |
	Units	1961–1990	B1	A1fi	B1	A1fi	B1	A1fi	B1	A1fi
Change in statewide avg temperatures										
Annual	°C	15.0	1.35	1.5	1.6	2.0	2.3	3.8	3.3	5.8
Summer (JJA)	°C	22.8	1.2	1.4	2.2	3.1	2.15	4.1	4.6	8.3
Winter (DJF)	°C	7.6	1.3	1.2	1.4	1.45	2.15	3.0	2.3	4.0
Change in statewide avg precipitation										
Annual	mm	544	−37	−51	+6	−70	+38	−91	−117	−157
Summer (JJA)	mm	20	−3	+2	−1	−7	+4	−46	−5	−1
Winter (DJF)	mm	269	−45	−55	+4	−44	+13	−13	−79	−92
Sea level rise	cm	—	8.7	9.5	11.6	12.7	19.2	28.8	26.8	40.9
Heatwave days										
Los Angeles	Days	12	28	35	24	36	44	76	47	95
Sacramento	Days	58	91	101	93	104	109	134	115	138
Fresno	Days	92	113	120	111	116	126	147	126	149
El Centro	Days	162	185	185	176	180	191	213	197	218
Length of heatwave season*	Days	115	135	142	132	141	149	178	162	204
Excess mortality for Los Angeles[†]										
Without acclimatization	avg no. of deaths/yr	—	—	—	—	—	394	948	667	1,429
With acclimatization	avg no. of deaths/yr	165	—	—	—	—	319	790	551	1,182
Change in April 1 snowpack SWE										
1,000–2,000 m elevation	%	3.6 km³	−60	−56	−58	−66	−65	−95	−87	−97
2,000–3,000 m elevation	%	6.5 km³	−34	−34	−24	−36	−22	−73	−75	−93
3,000–4,000 m elevation	%	2.3 km³	−11	−15	4	−16	15	−33	−48	−68
All elevations	%	12.4 km³	−38	−37	−26	−40	−29	−73	−72	−89
Change in annual reservoir inflow[‡]										
Total	%	21.7 km³	−18	−22	5	−10	12	−29	−24	−30
Northern Sierra	%	15.2 km³	−19	−22	3	−9	9	−29	−20	−24
Southern Sierra	%	6.5 km³	−16	−23	10	−14	17	−30	−33	−43
Change in April–June reservoir inflow[‡]										
Total	%	9.1 km³	−20	−24	−11	−19	−1	−46	−41	−54
Northern Sierra	%	5.5 km³	−21	−24	−16	−19	−6	−45	−34	−47
Southern Sierra	%	3.6 km³	−18	−24	−2	−19	5	−47	−52	−65
Change water year flow centroid[‡]										
Total	Days	03/26	0	2	−15	−7	−7	−14	−23	−32
Northern Sierra	Days	03/13	0	3	−16	−5	−3	−11	−18	−24
Southern Sierra	Days	05/01	−10	−7	−19	−12	−22	−34	−34	−43

avg, average; JJA, June, July, August; DJF, December, January, February; SWE, snow water equivalent.
*The number of days between the beginning of the year's first and end of the year's last heatwave.
[†]Reference period is 1990–1999, and projections are for the period 2090–2099.
[‡]Results are for inflows to seven major dams and reservoirs in the Sacramento/San Joaquin water system, including three in the Northern Sierra (Shasta, Oroville, and Folsom) and four in the Southern Sierra (New Melones, New Don Pedro, Lake McClure, and Pine Flat).

tation from the reference period were rescaled by simple monthly regression relations to ensure that the overall probability distributions of the simulated daily values closely approximated the observed probability distributions at selected long-term weather stations (7). The same regression relations were then applied to future simulations, such that rescaled values share the weather statistics observed at the selected stations. At the daily scales addressed by this method, the need to extrapolate beyond the range of the historically observed parts of the probability distributions was rare even in the future simulations (typically <1% of the future days) because most of the climate changes involve more frequent warm days than actual truly warmer-than-ever-observed days (7).

Except where otherwise noted, we present projected climate anomalies and impacts averaged over 2020–2049 (with a midpoint of 2035) and 2070–2099 (here designated as end-of-century, with a midpoint of 2085), relative to a 1961–1990 reference period.

Temperature. All simulations show increases in annual average temperature before midcentury that are slightly greater under the higher A1fi emissions scenario (see Fig. 4, which is published as supporting information on the PNAS web site). By end-of-century, projected temperature increases under A1fi are nearly twice those under B1, with the more sensitive HadCM3 model producing larger absolute changes (Table 1). Downscaled seasonal mean temperature projections (10) show consistent spatial patterns across California, with lesser warming along the southwest coast and increasing warming to the north and northeast (Fig. 1). Statewide, the range in projected average temperature increases is higher than previously reported (11–14), particularly for summer temperature increases that are equal to or greater than increases in winter temperatures.
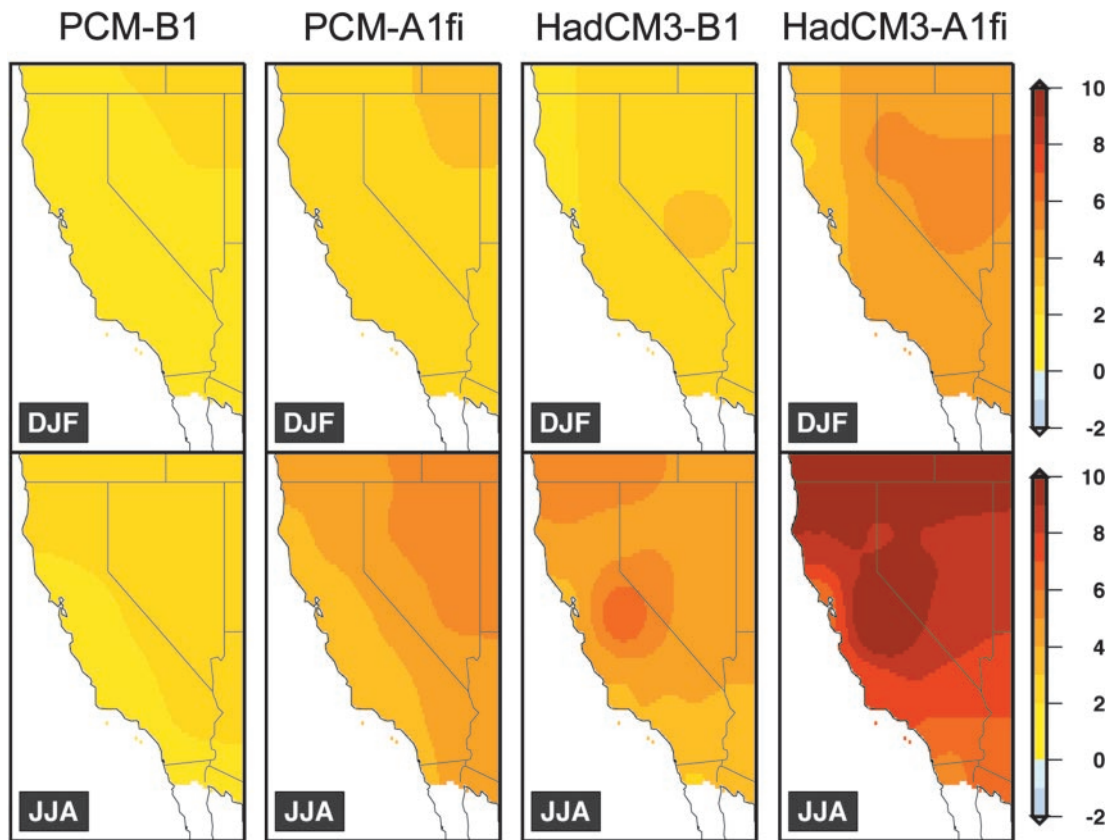
Fig. 1. Downscaled winter (DJF) and summer (JJA) temperature change (°C) for 2070–2099, relative to 1961–1990 for a 1/8° grid. Statewide, SRES B1 to A1fi winter temperature projections for the end of the century are 2.2–3°C and 2.3–4°C for PCM and HadCM3, respectively, compared with previous projections of 1.2–2.5°C and 3–3.5°C for PCM and HadCM2, respectively. End-of-century B1 to A1fi summer temperature projections are 2.2–4°C and 4.6–8.3°C for PCM and HadCM3, respectively, compared with previous projections of 1.3–3°C and 3–4°C for PCM and HadCM2, respectively (11–14).

Precipitation. Precipitation shows a tendency toward slight decreases in the second half of the century with no obvious interscenario differences in magnitude or frequency (see Figs. 5–10, which are published as supporting information on the PNAS web site). Three of four simulations project winter decreases of −15% to −30%, with reductions concentrated in the Central Valley and along the north Pacific Coast. Only PCM B1 projects slight increases (≈7%) by the end of the century (Table 1). These results differ from previous projections showing precipitation increases of 75–200% by 2100 (11–13), but they are consistent with recent PCM-based midrange projections (14, 15). The larger-scale pattern of rainfall over North America is more uniform across scenarios, showing an area of decreased (or lesser increase in) precipitation over California that contrasts with increases further up the coast (see Fig. 11, which is published as supporting information on the PNAS web site). Because interdecadal variability often dominates precipitation over California, projected changes in climate and impacts associated with the direct effects of temperature should be considered more robust than those determined by interactions between temperature and precipitation or precipitation alone.

Extreme Heat and Heat-Related Mortality

Temperature extremes increase in both frequency and magnitude under all simulations, with the most dramatic increases occurring under the A1fi scenario. Changes in local temperature extremes were evaluated based on exceedance probability analyses, by using the distribution of daily maximum temperatures downscaled to representative locations (16). Exceedance probabilities define a given temperature for which the probability exists that X% of days throughout the year will fall below that temperature (i.e., if the 35°C exceedance probability averages 95% for the period 2070–2099, this means that an average of 95% or ≈347 days per year are likely to lie below 35°C). For the four locations examined for extreme heat occurrence (Los Angeles, Sacramento, Fresno, and Shasta Dam), mean and maximum temperatures occurring 50% and 5% of the year increase by 1.5–5°C under B1 and 3.5–9°C under A1fi by the end of the century. Extreme temperatures experienced an average of 5% of the year during the historical period are also projected to increase in frequency, accounting for 12–19% (B1) and 20–30% (A1fi) of days annually by 2070–2099 (see Fig. 12, which is published as supporting information on the PNAS web site).

The annual number of days classified as heatwave conditions (3 or more consecutive days with temperature above 32°C) increases under all simulations, with more heatwave days under A1fi before midcentury (see Fig. 13, which is published as supporting information on the PNAS web site). Among the four locations analyzed, increases and interscenario differences are proportionally greatest for Los Angeles, a location that currently experiences relatively few heatwaves. By the end of the century, the number of heatwave days in Los Angeles increases four times under B1, and six to eight times under A1fi. Statewide, the length of the heatwave season increases by 5–7 weeks under B1 and by 9–13 weeks under A1fi by the end of this century, with interscenario differences emerging by midcentury (Table 1; see also Fig. 14, which is published information on the PNAS web site).

The connection between extreme heat and summer excess mortality is well established (17). Heat-related mortality estimates for the Los Angeles metropolitan area were determined
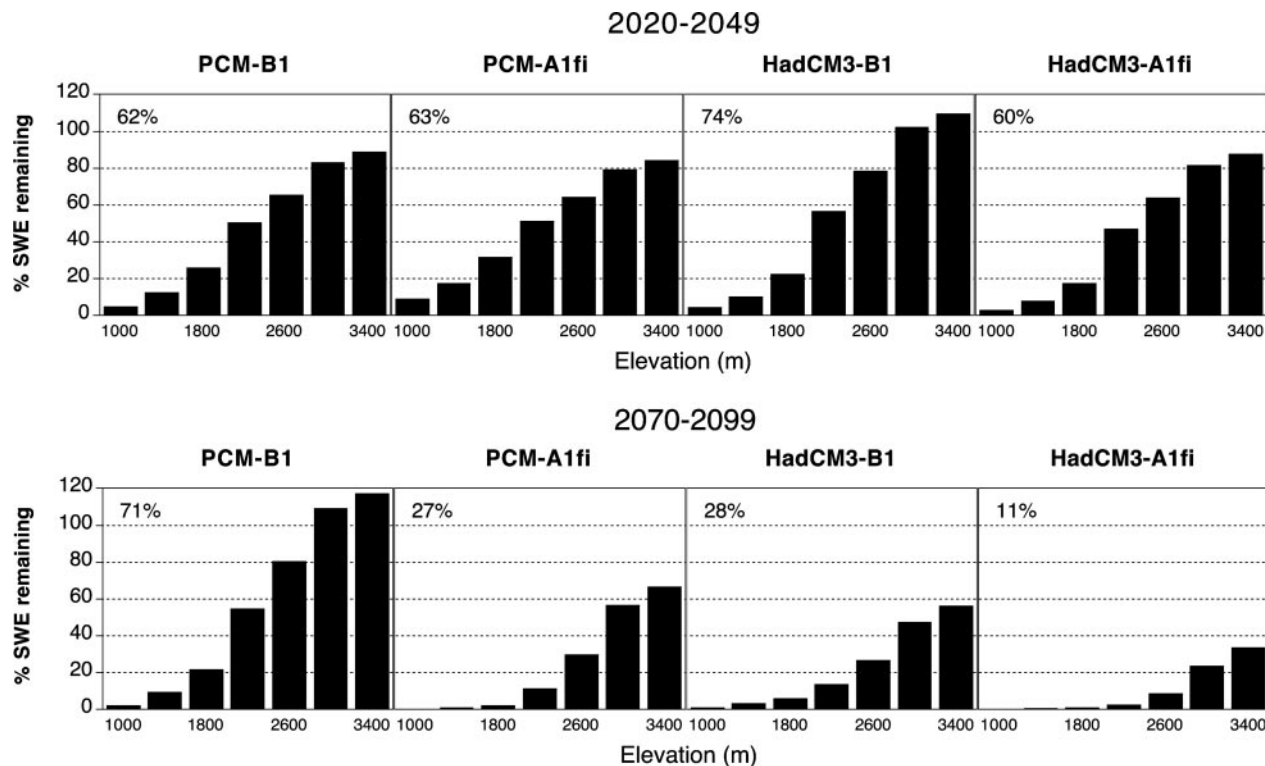
2020–2049

2070–2099

Fig. 2. Average snowpack SWE for 2020–2049 and 2070–2099 expressed as a percent of the average for the reference period 1961–1990 for the Sierra Nevada region draining into the Sacramento–San Joaquin river system. Total SWE losses by the end of the century range from 29–72% for the B1 scenario to 73–89% for the A1fi scenario. Losses are greatest at elevations below 3,000 m, ranging from 37–79% for B1 to 81–94% for A1fi by the end of the century. Increases in high elevation SWE for midcentury HadCM3 B1 and end-of-century PCM B1 runs result from increased winter precipitation in these simulations.

by threshold meteorological conditions beyond which mortality tends to increase. An algorithm was developed to determine the primary environmental factors (including maximum apparent temperature, number of consecutive days above the threshold apparent temperature, and time of year) that explain variability in excess mortality for all days with apparent maximum temperatures at or above the derived daily threshold apparent temperature (18) value of 34°C (see *Heat-Related Mortality* in *Supporting Text*). Estimates do not account for changes in population or demographic structure.

From a baseline of ≈165 excess deaths during the 1990s, heat-related mortality in Los Angeles is projected to increase by about two to three times under B1 and five to seven times under A1fi by the 2090s if acclimatization is taken into account (see *Heat-Related Mortality* in *Supporting Text*). Without acclimatization, these estimates are about 20–25% higher (Table 1). Actual impacts may be greater or lesser depending in part on demographic changes and societal decisions affecting preparedness, health care, and urban design. Individuals likely to be most affected include elderly, children, the economically disadvantaged, and those who are already ill (19, 20).

Impacts on Snowpack, Runoff, and Water Supply

Rising temperatures, exacerbated in some simulations by decreasing winter precipitation, produce substantial reductions in snowpack in the Sierra Nevada Mountains, with cascading impacts on California winter recreation, streamflow, and water storage and supply. Snowpack SWE was estimated by using daily, bias-corrected and spatially downscaled temperature and precipitation to drive the Variable Infiltration Capacity distributed land surface hydrology model. The Variable Infiltration Capacity model, using the resolution and parameterization also implemented in this study, has been shown to reproduce observed

streamflows when driven by observed meteorology (10) and has been applied to simulate climate change (8) in this region. April 1 SWE decreases substantially in all simulations before midcentury (see Fig. 15, which is published as supporting information on the PNAS web site). Reductions are most pronounced at elevations below 3,000 m, where 80% of snowpack storage currently occurs (Table 1 and Fig. 2). Interscenario differences emerge before midcentury for HadCM3 and by the end of the century for both models. These changes will delay the onset of and shorten the ski season in California (see *Impact of Decreasing Snowpack on California's Ski Industry* in *Supporting Text*).

Water stored in snowpack is a major natural reservoir for California. Differences in SWE between the B1 and A1fi scenarios represent ≈1.7 km³ of water storage by midcentury and 2.1 km³ by the end of the century for HadCM3. For PCM, overall SWE losses are smaller, but the difference between the A1fi and B1 scenarios is larger by the end of the century, representing >4 km³ of storage. Reductions for all simulations except PCM under the lower B1 emission scenario are greater than previous projections of diminishing snowpack for the end of the century (8, 21). By 2020–2049 the SWE loss is comparable to that previously projected for 2060 (22).

Warmer temperatures and more precipitation falling as rain instead of snow also causes snowmelt runoff to shift earlier under all simulations (Table 1), which is consistent with earlier studies (23). The magnitude of the shift is greater in the higher-elevation Southern basins and under the higher A1fi scenario. Stream inflows to major reservoirs decline because of diminished snowpack and increased evaporation before midcentury, except where winter precipitation increases (Table 1). The greater reductions in inflows seen under A1fi are driven by both higher temperatures and lower average precipitation as compared with B1.
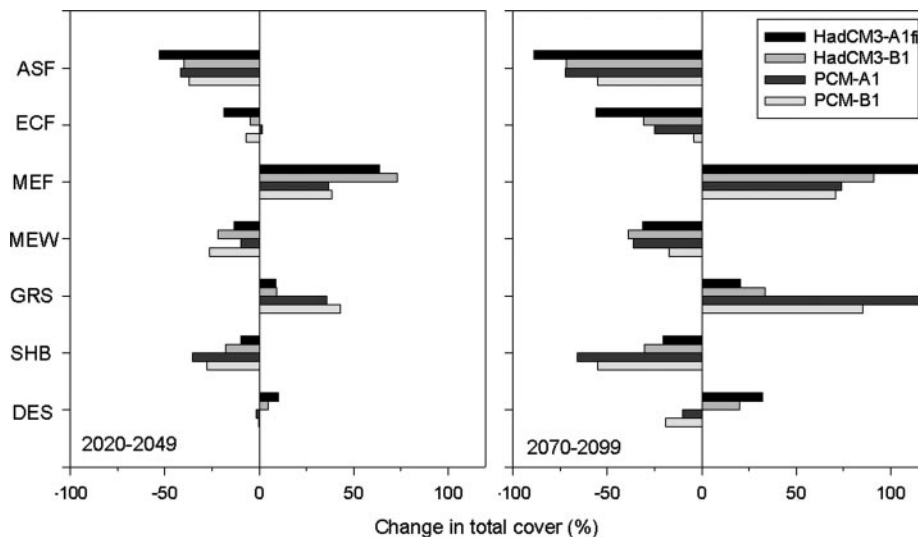
Fig. 3. Statewide change in cover of major vegetation types for 2020–2049 and 2070–2099, relative to simulated distributions for the 1961–1990 reference period. ASF, alpine/subalpine forest; ECF, evergreen conifer forest; MEF, mixed evergreen forest; MEW, mixed evergreen woodland; GRS, grassland; SHB, shrubland; DES, desert. Increasing temperatures drive the reduction in alpine/subalpine forest cover and cause mixed conifer forest to displace evergreen conifer forest in the Sierra Nevada Mountains and the North Coast. Mixed conifer forest in the South Coast expands because of increased humidity and reduced fire frequency. Because of drier conditions and increased fire frequency in inland locations, grassland displaces shrubland and woodland, particularly in the PCM simulations, whereas warmer and drier conditions under HadCM3 cause an expansion of desert cover in the southern Central Valley.

Earlier runoff may also increase the risk of winter flooding (7). Currently, state operators maintain ≈12 km³ of total vacant space in the major reservoirs to provide winter and early spring flood protection,[n] a volume approximately equal to that stored in the natural snowpack reservoir by April 1st. Capturing earlier runoff to compensate for future reductions in snowpack would take up most of the flood protection space, forcing a choice between winter flood prevention and maintaining water storage for the summer and fall dry period use. Flood risk and freshwater supply are also affected by higher sea levels, which are projected to rise 10–40 cm under B1 and 20–65 cm under A1fi by 2100 (Table 1; see also Fig. 16, which is published as supporting information on the PNAS web site).

Declining Sierra Nevada snowpack, earlier runoff, and reduced spring and summer streamflows will likely affect surface water supplies and shift reliance to groundwater resources, already overdrafted in many agricultural areas in California (24). This could impact 85% of California's population who are agricultural and urban users in the Central Valley, San Francisco Bay Area, and the South Coast, about half of whose water is supplied by rivers of the Central Valley. Under A1fi (both models) and B1 (HadCM3), the projected length, frequency, and severity of extreme droughts in the Sacramento River system during 2070–2099 substantially exceeds what has been experienced in the 20th century. The proportion of years projected to be dry or critical increases from 32% in the historical period to 50–64% by the end of the century under all but the wetter PCM B1 scenario (see Table 2, which is published as supporting information on the PNAS web site). Changes in water availability and timing could disrupt the existing pattern of seniority in month-dependent water rights by reducing the value of rights to mid- and late-season natural streamflow and boosting the value of rights to stored water. The overall magnitude of impacts on water users depends on complex interactions between temperature-driven snowpack decreases and runoff timing, precipita-

tion, future population increases, and human decisions regarding water storage and allocation (see *Impacts on Water Supply* in *Supporting Text*).

Impacts on Agriculture and Vegetation Distribution

In addition to reductions in water supply, climate change could impact California agriculture by increasing demand for irrigation to meet higher evaporative demand, increasing the incidence of pests (25), and through direct temperature effects on production quality and quantity. Dairy products (milk and cream, valued at $3.8 billion annually) and grapes ($3.2 billion annually) are the two highest-value agricultural commodities of California's $30 billion agriculture sector (26). Threshold temperature impacts on dairy production and wine grape quality were calculated by using downscaled temperature projections for key counties, relative to average observed monthly temperatures.[o]

For dairy production, losses were estimated for temperatures above a 32°C threshold (27), as well as for additional losses between 25°C (28) and 32°C. For the top 10 dairy counties in the state (which account for 90% of California's milk production), rising temperatures were found to reduce production by as much as 7–10% (B1) and 11–22% (A1fi) by the end of the century (see Table 3, which is published as supporting information on the PNAS web site). Potential adaptations may become less practical with increasing temperature and humidity (29).

For wine grapes, excessively high temperatures during ripening can adversely affect quality, a major determinant of market value. Assuming ripening occurs at between 1,150 and 1,300 biologically active growing degree days (30), ripening month was determined by summing modeled growing degree days above 10°C from April to October, for both baseline and projected scenarios. Monthly average temperature at the time of ripening was used to estimate potential temperature impacts on quality. For all simulations, average ripening occurs 1–2 months earlier and at higher temperatures, leading to degraded quality and marginal/impaired conditions for all but the cool coastal region

---

[n]See the U.S. Army Corps of Engineers Flood Control Requirements for California Reservoirs, Sacramento District Water Control Data System, Sacramento, CA (www.spk-wc.usace.army.mil).

[o]See Western U.S. Climate Historical Summaries (Western Regional Climate Center) at www.wrcc.dri.edu/climsum.html.

Hayhoe *et al.*

under all scenarios by the end of the century (see Table 3, which is published as supporting information on the PNAS web site). As with other perennial crops, adaptation options to shift varieties or locations of production would require significant time and capital investment.

The distribution of California's diverse vegetation types also changes substantially over the century relative to historical simulations (Fig. 3; see also Fig. 17, which is published as supporting information on the PNAS web site). Projections of changes in vegetation distribution are those given by MC1, a dynamic general vegetation model that simulates climate-driven changes in life-form mixtures and vegetation types; ecosystem fluxes of carbon, nitrogen, and water; and fire disturbance over time (31). Vegetation shifts driven primarily by temperature, such as reductions in the extent of alpine/subalpine forest and the displacement of evergreen conifer forest by mixed evergreen forest, are consistent across models and more pronounced under A1fi by the end of the century. Changes driven by precipitation and changes in fire frequency are model-dependent and do not exhibit consistent interscenario differences. Most changes are apparent before mid-century, with the exception of changes in desert cover. The shift from evergreen conifer to mixed evergreen forest and expansion of grassland are consistent with previous impact analyses (13), whereas the extreme reduction in alpine/subalpine forest and expansion of desert had not been reported in previous impacts assessments (12, 13).

Conclusions

Consistent and large increases in temperature and extreme heat drive significant impacts on temperature-sensitive sectors in California under both lower and higher emissions scenarios, with the most severe impacts occurring under the higher A1fi scenario. Adaptation options are limited for impacts not easily controlled by human intervention, such as the overall decline in snowpack and loss of alpine and subalpine forests. Although interscenario differences in climate impacts and costs of adaptation emerge mainly in the second half of the century, they are largely entrained by emissions from preceding decades (32). SRES scenarios do not explicitly assume climate-specific policy intervention, and thus this study does not directly address the contrast in impacts due to climate change mitigation policies. However, these findings support the conclusion that climate change and many of its impacts scale with the quantity and timing of greenhouse gas emissions (33). As such, they represent a solid starting point for assessing the outcome of changes in greenhouse gas emission trajectories driven by climate-specific policies (32, 34), and the extent to which lower emissions can reduce the likelihood and thus risks of ''dangerous anthropogenic interference with the climate system'' (35).

1. Nakićenović, N., Alcamo, J., Davis, G., de Vries, B., Fenhann, J., Gaffin, S., Gregory, K., Grübler, A., Jung, T. Y., Kram, T., *et al.* (2000) *Intergovernmental Panel on Climate Change Special Report on Emissions Scenarios* (Cambridge Univ. Press, Cambridge, U.K.).
2. Parry, M. (2002) *Global Environ. Change* **12** (3)**,** 149–153.
3. Washington, W. M., Weatherly, J. W., Meehl, G. A., Semtner, A. J., Bettge, T. W., Craig, A. P., Strand, W. G., Arblaster, J., Wayland, V. B., James, R. & Zhang, Y. (2000) *Clim. Dyn.* **16,** 755–774.
4. Gordon, C., Cooper, C., Senior, C. A., Banks, H., Gregory, J. M., Johns, T. C., Mitchell, J. F. B. & Wood, R. A. (2000) *Clim. Dyn.* **16,** 147–168.
5. Pope, V. D., Gallani, M. L., Rowntree, P. R. & Stratton, R. A. (2000) *Clim. Dyn.* **16,** 123–146.
6. Wood, A. W., Maurer, E. P., Kumar, A. & Lettenmaier, D. P. (2002) *J. Geophys. Res.* **107,** 4429, 10.1029/2001JD000659.
7. Dettinger, M. D., Cayan, D. R., Meyer, M. K. & Jeton, A. E. (2004) *Clim. Change* **62,** 283–317.
8. VanRheenan, N. T., Wood, A. W., Palmer, R. N. & Lettenmaier, D. P. (2004) *Clim. Change* **62,** 257–281.
9. Wood, A. W., Leung, L. R., Sridhar, V. & Lettenmaier, D. P. (2004) *Clim. Change* **62,** 189–216.
10. Maurer, E. P., Wood, A. W., Adam, J. C., Lettenmaier, D. P. & Nijssen, B. (2002) *J. Clim.* **15,** 3237–3251.
11. Field, C. B., Daily, G. C., Davis, F. W., Gaines, S., Matson, P. A., Melack, J. & Miller, N. L. (1999) *Confronting Climate Change in California: Ecological Impacts on the Golden State* (Union of Concerned Scientists, Cambridge, MA, and Ecological Society of America, Washington, DC).
12. Wilkinson, R., Clarke, K., Goodchild, M., Reichman, J. & Dozier, J. (2002) *The Potential Consequences of Climate Variability and Change for California: The California Regional Assessment* (U.S. Global Change Research Program, Washington, DC).
13. Wilson, T., Williams, L., Smith, J. & Medelsohn, R. (2003) *Global Climate Change and California: Potential Implications for Ecosystems, Health, and the Economy*, Publication No. 500-03-058CF (California Energy Commission, Public Interest Energy Research Environmental Area, Sacramento).
14. Leung, L. R., Qian, Y., Bian, X., Washington, W. M., Han, J. & Roads, J. O. (2004) *Clim. Change* **62,** 75–113.
15. Snyder, M. A., Bell, J. L., Sloan, L. C., Duffy, P. B. & Govindasamy, B. (2002) *Geophys. Res. Lett.* **29,** 1514–1517.
16. Miller, N. L., Bashford, K. E. & Strem, E. (2003) *J. Am. Water Resour. Assoc.* **39,** 771–784.
17. Kalkstein, L. S. & Davis, R. E. (1989) *Ann. Assoc. Am. Geogr.* **79,** 44–64.
18. Watts, J. D. & Kalkstein, L. S. (2004) *J. Appl. Meteorol.* **43,** 503–513.
19. McGeehin, M. A. & Mirabelli, M. (2001) *Environ. Health Perspect.* **109,** 185–189.
20. Chestnut, L. G., Breffle, W. S., Smith, J. B. & Kalkstein, L. S. (1998) *Environ. Sci. Policy* **1,** 59–70.
21. Knowles, N. & Cayan, D. R. (2002) *Geophys. Res. Lett.* **29,** 1891–1895.
22. Knowles, N. & Cayan, D. R. (2004) *Clim. Change* **62,** 319–336.
23. Gleick, P. H. & Chalecki, E. L. (1999) *J. Am. Water Resour. Assoc.* **35,** 1429–1441.
24. California Department of Water Resources, Division of Planning and Local Assistance (1998) *Bulletin 160–98: California Water Plan* (California Department of Water Resources, Sacramento).
25. Harrington, R. & Stork, N. E., eds. (1995) *Insects in a Changing Environment* (Academic, London).
26. California Agricultural Statistics Service (2002) *California Agriculture Statistical Review* (California Agricultural Statistics Service, Sacramento).
27. Ahmed, M. M. M. & El Amin, A. I. (1997) *J. Arid Environ.* **35,** 737–745.
28. Mellado, M. (1995) *Veterinaria* **26,** 389–399.
29. Pittock, B., Wratt, D., Basher, R., Bates, B., Finlayson, M., Gitay, H., Woodward, A., Arthington, A., Beets, P., Biggs, B., *et al.* (2001) in *Climate Change 2001: Impacts, Adaptation, and Vulnerability* (Cambridge Univ. Press, Cambridge, U.K.).
30. Gladstones, J. (1992) *Viticulture and Environment* (Winetitles, Underdale, South Australia), 310 pp.
31. Lenihan, J., Drapek, R., Bachelet, D. & Neilson, R. (2003) *Ecol. Appl.* **13,** 1667–1681.
32. Swart, R., Mitchell, J., Morita, T. & Raper, S. (2002) *Global Environ. Change* **12,** 155–165.
33. Houghton, J. T., Ding, Y., Griggs, D. J., Noguer, M., van der Linden, P. J. & Xiaosu, D., eds. (2001) *Climate Change 2001: The Scientific Basis* (Cambridge Univ. Press, Cambridge, U.K.).
34. Arnell, N. W., Livermore, M. J. L., Kovats, S., Levy, P. E., Nicholls, R., Parry, M. L. & Gaffin, S. R. (2004) *Global Environ. Change* **14,** 3–20.
35. United Nations (1992) *United Nations Framework Convention on Climate Change* (United Nations, Rio de Janeiro, Brazil).

APPLIED PHYSICAL SCIENCES

ECOLOGY

Supporting Text

Emissions Scenarios

The Intergovernmental Panel on Climate Change's latest suite of emission scenarios, known as SRES (Special Report on Emissions Scenarios) (1), describe internally consistent pathways of future greenhouse gas emissions. SRES scenarios cover a wide range of alternative futures based on projections of economic growth, technology, energy intensity, and population. The SRES scenarios are not assigned probabilities, but rather can be viewed as possible futures, with the actual path depending on technology, economic development, and political will. The B1 and A1fi scenarios used in this study bracket the range of SRES scenarios, and they can be thought of as lower and higher bounds that encompass most, but not all, potential nonintervention emissions futures. Both scenarios follow similar demographic trends, with global population peaking in midcentury and then declining. Both also involve rapid technological development. At the higher end, however, economic growth and globalization lead to increases in energy use and industrial production, with much of the technological development being focused on fossil energy sources. This causes A1fi CO_2 emissions to climb throughout the century, reaching almost 30 Gt/year or six times 1990 levels by 2100 (2). Emissions under the B1 scenario are lower, based on a world that transitions relatively rapidly to service and information economies and that emphasizes the development of clean, nonfossil technology. CO_2 emissions in the B1 scenario peak at just below 10 Gt/year, around two times 1990 levels, at mid-century and decline slowly to below current-day levels. For comparison with mid-range business-as-usual projections used by previous studies (3-6), the temperature and precipitation projections provided here (Figs. 4 and 5) also include those corresponding to the mid-range A2 and B2 scenarios. Emissions and hence temperature projections for these scenarios fall between those of A1fi and B1, but underlying assumptions are very different. A2 describes a very heterogeneous world where economic development is regionally oriented and economic growth and technological change are relatively slow, whereas in B2 the emphasis is on local solutions to economic, social, and environmental sustainability with less rapid and more diverse technological change.

Precipitation

Projections of change in precipitation over California from the higher, lower, and two mid-range scenarios for both models tend to decrease, with most end-of-century projections falling between 0 and −1 mm/day. The full range varies between a net increase of +0.25 mm/day (PCM B1) to a decrease of −1 mm/day (HadCM3 A1fi) (Figs. 5 and 6). In general, precipitation appears to be dominated by interdecadal variability rather than long-term trends (Fig. 5). However, both models and scenarios do exhibit a consistent continental-scale pattern of increased precipitation along the upper Pacific

coast, with little change, generally a drying, over California by the end of the century (Fig. 11). In terms of extreme precipitation, the number of very wet days, indicated by nonexceedence probabilities of 95% at selected stations across California, decreases by 2–5% or 7–18 days per year (Fig. 7). Analysis of heavy rainfall events lasting 1, 4, and 7 days show a slight decrease in frequency over northern California and little change in southern California for HadCM3 projections (Fig. 8). In contrast, PCM projections suggest a possible increase in heavy precipitation events, particularly for the wetter B1 scenario, for shorter 24-hr events, and for southern California. Overall, changes in precipitation exceedance probabilities and heavy precipitation event frequencies show little significant trend, a result consistent with the lack of observed historical trend over the past century (7). Extreme dry periods are not projected to change significantly in either length or duration (Figs. 9 and 10). However, there is some indication that events on the order of a few weeks may become more frequent in the future, particularly for northern California (approximately one to two additional events per year for 2-week dry periods).

Extreme Heat

A measure of the projected change in maximum temperature extremes (8) is given by the shift in the 50% (mean maximum daily temperature) and the 95% (5% highest mean maximum daily temperatures for each 30-year period or roughly 18 days/year with temperatures exceeding this amount) nonexceedance values. The maximum daily temperature (T_x) exceedence probabilities at Shasta Dam, Los Angeles, Sacramento, and Fresno for emission scenarios A1fi and B1 using PCM and HadCM3 projections are shown in Fig. 12. The end-of-century change in 50% and 95% T_x exceedence probabilities for Shasta Dam are each greater than 7°C for the HadCM3 A1fi scenario and 6°C for the PCM A1fi scenario. Fresno also has shifts in T_x exceedence greater than 6°C for both scenarios. The 1961-1990 baseline 95% exceedence becomes the 70% and 75% exceedence values for HadCM3 and PCM A1fi, and 82% and 84% exceedence values for B1. Such shifts indicate that Fresno's historic 5% warmest days may occur as frequently as 25–30% of the year for A1fi and 16–18% for B1 by the end of this century. Other inland sites follow this increase in the number of warm days.

Exceedance probabilities can also be used to measure the number of days on which temperatures exceed a standardized threshold of 32°C (Fig. 12). By the end of the century (2070-2099), Los Angeles is projected to see such temperatures on as many as 110 days/year under the A1fi scenario, with a 33- to 44-day difference between emissions scenarios, a dramatic increase over the 22 days/year experienced during the reference period. Other locations are projected to experience less dramatic but substantial increases in extreme heat frequency.

Extreme heat can also be represented by changes in the length of the heatwave season and the number of days classified as heatwave conditions (here defined as 3 or more consecutive days with temperatures exceeding 32°C). The lengthening of future heat wave seasons is primarily due to earlier onset, with the season beginning 25-40 days earlier under B1, and twice that (50-80 days earlier) under the A1fi scenario (Fig. 14). Increases in the number of heatwave days under the B1 scenario are similar across most locations, ranging from 27-58 days/year (Fig. 13). Under A1fi, 49-83 more heatwave days are seen, which represents an increase of ~20-30 more days than under the B1 scenario. Proportionally greater increases are seen for Los Angeles, which currently experiences the lowest occurrence of heatwave days per year (12, as opposed to 60-160 for other locations).

Heat-Related Mortality

The mortality estimates derived for the B1 and A1fi 2090 scenarios were developed for the Los Angeles metropolitan area by using procedures that determine threshold meteorological conditions beyond which mortality tends to increase. Meteorologically "oppressive" conditions are determined by identifying maximum *apparent temperature* thresholds that have been historically associated with rising heat-related mortality. Apparent temperature is a combination of the impacts of temperature, relative humidity, and windspeed on the human body, and it can be considered an adequate surrogate to evaluate heat transfer effects on humans (9). Relating daily human mortality to daily maximum apparent temperature values, a threshold apparent temperature value was determined for Los Angeles of 34°C. When reached or exceeded, this daily apparent temperature threshold yields a mean mortality value that is statistically significantly higher than the long-term mean at a 0.05 level of significance.

An algorithm was developed for all days with maximum apparent temperatures at or above 34°C to determine the environmental factors most responsible for explaining the variability in mortality during oppressive weather. Both meteorological (maximum and minimum apparent temperature and dewpoint, cloud cover, and others) and nonmeteorological (consecutive days of oppressive weather and time of season when oppressive weather occurs) variables are potential dependent variables within this algorithm, which can be used to estimate daily heat-related mortality. The final algorithm ($P < 0.001$) is:

$$Mort_p = -8.481 + 0.326AT + 1.891CD - 0.012TS,$$

where estimated daily mortality ($Mort_p$) is given as a function of maximum apparent daily temperature (AT), the day's position in a consecutive sequence of days with maximum apparent temperature equal to or exceeding 34°C (CD), and days after May 1 (TS).

The impact of acclimatization was determined by using a procedure that we deem superior to the previously common "analog city" approach (10). The new acclimatization procedure assumes that people will most likely respond to heat under climate change conditions as they do today during the very hottest summers. Thus, instead of choosing analog cities, which possess different demographics and urban structure than the target city, we have selected "analog summers" in the target city that best duplicate the summers as expressed in the climate change scenarios. For Los Angeles, the five hottest summers over the past 24 years were selected based on mean summer apparent temperature values. A new algorithm was developed for days during the hottest summers that equaled or exceeded the apparent temperature threshold of 34°C. The algorithm is:

$$Mort_p = -4.774 + 0.178AT + 1.928CD - 0.013TS.$$

As expected, the new algorithm for the hottest summers shows a decreased sensitivity to the heat because of intraseasonal acclimatization (this is apparent in the lower coefficient for the AT variable). By using the new algorithm, revised mortality totals were derived. Under acclimatization, mortality totals averaged on the order of 15–20% lower than those yielded by the original algorithm (see Table 1). This is our best estimate for acclimatized mortality in Los Angeles under the two given climate change scenarios.

Impact of Decreasing Snowpack on California's Ski Industry

Projections of decreases in Sierra snowpack (Fig. 15) have the potential to substantially affect California's ski industry. Most of California's 34 ski resorts are based between 2,000–2,500 m with a vertical rise of ~800–1,200 m. For these elevations, we use a conservative estimate of a 50 mm minimum SWE threshold to define the beginning of the ski season. This lower bound corresponds to 200–500 mm or only 1–2 ft of snow depth under typical snow densities (11). This value is taken as the range of minimum snow required for ski slope operation for some resorts, although a higher range of 2–4 ft may be a more accurate average for California ski resorts in general (B. Roberts, California Ski Industry Association, personal communication).

For the reference period 1961-1990, the beginning of the snow season tends to fall during the last week of November, and it lasts until late June. Under all scenarios, the ski season is found to shorten, with the majority of the change being an earlier melt date. However, the delay in the start of the ski season is sufficient to suggest likely impacts on the economic vitality of the ski industry, as there is a general reliance for successful operations on snow cover in ski areas by mid December (B. Roberts, California Ski Industry Association, personal communication). For PCM simulations, by the end of the century the start of the ski season is delayed by 22 (B1) to 29 (A1fi) days and is 49–103 days shorter. Under the HadCM3, similar delays occur by mid-century, and by the end of

the century, the ski season begins 36 days later under B1, while the 50-mm threshold is never crossed under the A1fi scenario (Fig. 15).

Costs of adaptation may include increased reliance on snowmaking and/or relocating or terminating operations. Relocation options may be limited, however, as many of the ski resorts in Oregon and Washington State are located at lower elevations than those in California. Mid-range PCM estimates show snowpack reductions of 63% for the Cascades and 40% for the entire Columbia River Basin, on the same order as reductions seen in California under similar projections (13), suggesting a net loss rather than shift in ski-related tourist income throughout the region.

Sea-Level Rise

Sea levels along the California coast are projected to continue to rise over the next century. Future rates of increase range from ≈10–43 cm/100 years for B1 to ≈18–64 cm/100 years for A1fi (Fig. 16), compared to the historical 17 cm/100 years rate of mean global sea-level rise (2). Higher sea levels would threaten many elements of California's social, economic, freshwater, and ecological systems (14). El Niño has produced some of the highest sea levels and winter storms with the highest coastal waves (15) observed in several decades of records along the California coast. The combination of such events with heightened mean sea level and increased diurnal tidal ranges (16) would expose the coast to severe flooding and erosion, damage to coastal structures and real estate, and salinity intrusion of vulnerable coastal aquifers. The San Francisco Bay and Delta are particularly vulnerable to rising sea levels, which may cause flooding of leveed islands, real estate, and wetlands as well as greater salt water intrusion into the North Bay and Delta. This would impact currently protected ecosystems as well as the fresh water supply in that region (17, 18).

Impacts on Water Supply

The ultimate impacts of climate change on water availability, timing, and supply for California are as much a function of the behavioral response of individuals and organizations as of hydrology. If snowmelt is used for storage, there is the potential for very little impact on supply, although with greatly reduced storage the risk of water shortages during dry years would increase. If used primarily for supply, reductions in available water from river sources could be almost as large as the projected decreases in April snowpack, which are greatest under the A1fi scenario.

Additional storage could be developed at some cost whether in the form of above-ground storage or aquifer-based conjunctive use. Without additional storage, even with higher runoff during some winter months it appears unlikely that the extra runoff could effectively be captured and retained for use after April 1 without reducing the amount of

flood storage space left in reserve on April 1. Besides flood storage in April, the amount of water that can be delivered from storage during the summer irrigation season is determined by the amount of water that needs to be left in storage at the end of the summer for carryover to protect against the possibility of drought in the following years. Both the need to leave empty storage for flood protection on April 1 and the need for carryover storage at the end of the summer reflect uncertainty about future weather conditions and risk aversion on the part of reservoir operators. To the extent that there might be an increase in the future variability of precipitation and streamflow, we would expect to see a greater need for precaution in reservoir management.

Changes in water availability and timing have important implications for water supply and management (19). The existing pattern of seniority in water rights could be disrupted by reducing the value of rights to mid- and late-season natural streamflow and boosting the value of rights to stored water. The degree to which users would be affected depends on how private surface water rights and contractual arrangements within the two major California water projects adapt to substantial changes in natural flow conditions. Senior users without access to storage, including many riparians and holders of water rights that predate the major projects, could face unprecedented shortages due to reduced summertime streamflow. Seventy-five percent of total water use currently occurs between April and September when lawns are being watered and crops are being grown. With existing weak controls on groundwater pumping, a probable response is increased groundwater pumping that could exacerbate existing overdraft in the San Joaquin Valley.

California identifies five types of water years, ranging from wet to critical, based on the amount of unimpaired runoff in the Sacramento and San Joaquin River systems. Table 2 shows the distribution of water year types for the Sacramento River system (the 40-30-30 Four River Index) over the historical period 1906-1999 together with the projected distribution of year types over the period 2070-2099 under alternative climate change scenarios. In the historical period, 31% of the years were dry or critical. Under PCM B1, the proportion of years projected to be dry or critical at the end of the century falls to about 8%, but under the other three scenarios (PCM A1fi, HadCM3 A1fi and B1) it rises to 50–64%. For the three drier scenarios, the frequency of the driest year on record over the last century increases 10-fold to approximately one time per decade by the end of the century.

Under the drier scenarios, the length, severity and frequency of extreme droughts, defined as occurring only once over the past hundred years for the Sacramento River system, could more than double with equal or greater water loss. The Sacramento River runoff averaged 22.1 km^3/year over the historical period and the lowest annual runoff recorded was 6.3 km^3/year in 1976. Over the period 2070-2099, 2 years are projected to have lower annual runoff than this under HadCM3 B1, and 3 years are projected to have lower annual runoff under PCM A1fi and HadCM3 A1fi, the lowest being a runoff of 4.4

km^3/year projected under HadCM3 A1fi. In the historical period, the worst 2-year drought occurred in 1976–1977 when the Sacramento River runoff averaged 8.1 km^3/year; other major droughts were 1929–1934, when the runoff averaged 12.1 km^3/year, and 1987–1992, when it averaged 12.3 km^3/year. Over the period 2070–2098, PCM A1fi projects a 4-year drought where the runoff averages 9.9 km^3/year and two 3-year droughts where it averages 7.2 and 11.8 km^3/year, respectively. HadCM3 A1fi projects a 14-year drought where the runoff averages 10.7 km^3/year, and HadCM3 B1 projects a 3-year drought where the runoff averages 8.5 km^3/year.

These estimates are likely to understate the severity of any future droughts or water shortages as they do not account for changes in climate variability (for example, there is some indication of increases in the frequency of dry periods on the order of 2 weeks; see "Precipitation" above). Despite population growth for the past 15-20 years, water withdrawals over the United States and California have been fairly constant as water use efficiency has increased (20). However, population growth in California is expected to double or even triple from its current population of 34 million by the end of the century (5), which is likely to increase water demand but is not accounted for in estimates of water impacts here.

Temperature Impacts on Agriculture

Increases in average and extreme temperatures due to climate change are likely to produce adverse effects on quantity and quality for a number of California's agricultural products, including dairy products and wine grapes. Milk production begins to decline at temperatures greater than 25°C (21), and Holsteins, the predominant breed in California, have demonstrated a 1.15 kg decline in daily milk production per degree over 32°C (22). Dairy production is currently concentrated in the south Central Valley, with 67% of 2002 dairy value originating in only five counties [Tulare, Merced, Stanislaus, San Bernardino, and Kings (23)]. High-end estimates of production loss over 25°C, which are probably more reflective of the temperature ranges found in California, show the largest production decline in the highest-producing counties for both HadCM3 scenarios, whereas PCM predicts a loss throughout California (Table 3). For the low-end estimates ($T > 32$°C), milk production is moderately reduced in both HadCM3 scenarios and negligible for both PCM scenarios. Statewide, production losses for the 25°C threshold range from −7 to −10% for the B1 scenario, but almost double to −11 to −22% for the A1fi scenario. Interscenario differences are even more pronounced for the 32°C threshold, where losses for B1 are minimal, at ~0.5–2.5% while A1fi shows losses of 2–8% of production value (Table 3). Potential adaptations include using shade and sprinklers to reduce heat stress (24), measures that can be cost-effective under some conditions but become less so with increasing temperature and humidity (25).

For most wine grape varieties, the average temperature should fall between 15°C and 21°C in the final month of ripening to produce high-quality wines; average monthly temperature exceeding 24°C nearly always reduce quality for most table wines, through the combined effects of heat and moisture stress (12). Under all simulations, the timing of grape harvest based on accumulated degree-days above 10°C beginning in April is expected to be an average of 1–2 months earlier in 2070-2099 relative to the reference period. This produces a shift from optimal to marginal and marginal to quality-impaired ripening temperatures across major grape-growing regions. By mid-century, all simulations show a slight shift to the warmer end of the optimal range in currently optimal grape-growing zones in the Wine Country (Sonoma and Napa Counties) and Cool Coastal (Monterey and Mendocino Counties) areas. By the end of the century, all simulations show a shift from optimal to marginal or impaired conditions in the Wine Country and the Central Coast (San Luis Obispo and Monterey Counties; see Table 3). All scenarios also show a shift from current marginal to impaired conditions for the Central Valley grape-growing regions by mid-century and beyond. By 2070–2099, even under the lower B1 scenario all regions become either marginal or impaired with the exception of the Cool Coastal region. Under the A1fi scenario, the majority of locations are impaired, suggesting significant economic impacts of modeled temperature increases for grape-growing regions throughout California.

Changes in Vegetation Distribution

Changes in vegetation distribution across California occur under all scenarios, as initial decreases in some vegetation types and increases in others that are first visible in 2020–2049 almost double by 2070–2099 (Fig. 17). Temperature-induced declines in Alpine/Subalpine forest (with almost total disappearance under HadCM3 A1fi) and major shifts from evergreen conifer forest to mixed evergreen conifer forest are fairly robust across models, increasing in magnitude from the B1 to A1fi scenarios. Under all simulations, wildfire plays a role in converting shrubland and woodland to grassland. Decreases in effective moisture shift the competitive balance in favor of the more drought-tolerant grasses, and increases in grass biomass provide more fine fuels that support more frequent fires. Increased fire favors grasses, which re-establish more rapidly than slower growing woody lifeforms after burning. The increase in grassland is much larger for the PCM than for the HadCM3 scenarios, highlighting the complexity of the fire-mediated changes driven not only by changes in the structure and loading of fuels with changes in effective moisture, but also by changes in temperature and humidity as they affect fuel moisture. The effect of the latter is also evident along the southern coast where increases in fuel moisture with increased humidity result in less fire and the consequent expansion of forest under the PCM scenarios. Declines in effective moisture under the warmer and drier HadCM3 scenarios reduce the productivity of both grass and woody lifeforms in the southern Central Valley, resulting in a significant expansion of desert. Under the PCM scenarios, more moderate declines in effective moisture trigger a

fire-mediated shift from desert scrub to arid grassland in this region of the state. The only areas to experience little change are the north part of the Central Valley, which remains grassland under all scenarios, and the Southeast, which remains desert.

1. Nakićenović, N., Alcamo, J., Davis, G., de Vries, B., Fenhann, J., Gaffin, S., Gregory, K., Grübler, A., Jung, T. Y., Kram, T., *et al.* (2000) *Intergovernmental Panel on Climate Change Special Report on Emissions Scenarios* (Cambridge Univ. Press, Cambridge, U.K.).

2. Houghton, J. T., Ding, Y., Griggs, D. J., Noguer, M., van der Linden, P. J. & Xiaosu D., (2001) *Climate Change 2001: The Scientific Basis. Contribution of Working Group I to the Third Assessment Report of the Intergovernmental Panel on Climate Change* (Cambridge Univ. Press, Cambridge, U.K.).

3. Field, C. B., Daily, G. C., Davis, F. W., Gaines, S., Matson, P. A., Melack, J. & Miller, N. L. (1999) *Confronting Climate Change in California: Ecological Impacts on the Golden State* (Union of Concerned Scientists, Cambridge, MA, and Ecological Society of America, Washington, DC)

4. Wilkinson, R., Clarke, K., Goodchild, M., Reichman, J. & Dozier, J. (2002) *The Potential Consequences of Climate Variability and Change for California: The California Regional Assessment* (U.S. Global Change Research Program, Washington, DC).

5. Wilson, T., Williams, L., Smith, J. & Medelsohn, R. (2003) *Global Climate Change and California: Potential Implications for Ecosystems, Health, and the Economy,* Publication No. 500-03-058CF (California Energy Commission, Public Interest Energy Research Environmental Area, Sacramento, CA).

6. Leung, L. R., Qian, Y., Bian, X., Washington, W. M., Han, J. & Roads, J. O. (2004). *Clim. Change* **62,** 75-113.

7. Kunkel, K. E. (2003) *Natural Hazards* **29** (2), 291-305.

8. Miller, N. L., Bashford, K. E., & Strem, E. (2003) *J. Am. Water Resour. Assoc.* **39,** 771-784.

9. Watts, J. D. & Kalkstein, L. S. (2004) *J. Appl. Met.* **43** (3), 503-513.

10. Kalkstein, L. S. & Greene, J. S. (1997) *Environ. Health Perspect.* **105** (1), 84-93.

11. Gray, D. M. & Male, D. H., eds. (1981) *Handbook of Snow* (Pergamon, New York).

12. Gladstones, J. (1992) *Viticulture and Environment* (Winetitles, Underdale, South Australia).

13. Payne, J. T., Wood, A. W., Hamlet, A. F., Palmer, R. N. & Lettenmaier, D. P. (2004) *Clim. Change* **62,** 233-256.

14. Scavia, D., Field, J. C., Boesch, D. F., Buddemeier, R. W., Burkett, V., Cayan, D. R., Fogarty, M., Harwell, M. A., Howarth, R. W., Mason, C., *et al*. (2002) *Estuaries* **25** (20), 149-164.

15. Bromirski, P. D., Flick, R. E. & Cayan, D. R. (2003) *J. Clim.* **16** (6), 982-993.

16. Flick, R. E., Murray, J. F. & Ewing, L. C. (2003) *J. Waterway Port Coastal Ocean Eng.* **129** (4), 155-164.

17. Knowles, N. & Cayan, D. R. (2004) *Clim. Change* **62,** 319-336.

18. Knowles, N. (2002) *Water Resour. Res.* **38,** Art. 1289.

19. Gleick, P. H. & Chalecki, E. L. (1999) *J. Am. Water Resour. Assoc.* **35,** 1429-1441.

20. Hutson, S. S., Barber, N. L., Kenny, J. F., Linsey, K. S., Lumia, D. S. & Maupin, M. A. (accessed May 2004) *Estimated Use of Water in the United States in 2000* (U.S. Geological Survey Circular 1268, http://water.usgs.gov/pubs/circ/2004/circ1268/).

21. Mellado, M. (1995) *Veterinaria* **26,** 389-399.

22. Ahmed, M. M. M. & El Amin, A. I. (1997) *J. Arid Environ.* **35,** 737-745.

23. California Agricultural Statistics Service (2002) *California Agriculture Statistical Review* (California Agricultural Statistics Service, Sacramento, CA).

24. Jones, R. N. & Hennessy, K. J. (2000) *Climate Change Impacts in the Hunter Valley: A Risk Assessment of Heat Stress Affecting Dairy Cattle* (Commonwealth Scientific and Industrial Research Organization Atmospheric Research, Aspendale, Victoria, Australia).

25. Pittock, B., Wratt, D., Basher, R., Bates, B., Finlayson, M., Gitay, H., Woodward, A., Arthington, A., Beets, P., Biggs, B., *et al*. (2001) *Climate Change 2001: Impacts, Adaptation, and Vulnerability* (Cambridge Univ. Press, Cambridge, U.K.).